EUROPEAN ORGANIZATION FOR NUCLEAR RESEARCH

CERN–EP-2000-035

14 February 2000

W pair production cross-section and W branching fractions in e^+e^- interactions at 189 GeV

DELPHI Collaboration

Abstract

The cross-section for the process $e^+e^- \to W^+W^-$ has been measured with the data sample collected by DELPHI at an average centre-of-mass energy of 189 GeV and corresponding to an integrated luminosity of 155 pb^{-1}. Based on the 2392 events selected as WW candidates, the cross-section for the doubly resonant process $e^+e^- \to W^+W^-$ has been measured to be 15.83 ± 0.38 (stat) $\pm$ 0.20 (syst) pb. The branching fractions of the W decay were also measured and found to be in good agreement with the Standard Model expectation. From these a value of the CKM mixing matrix element $|V_{cs}| = 1.001 \pm 0.040$ (stat) $\pm$ 0.020 (syst) was derived.

Accepted by Physics Letters B

P.Abreu[22], W.Adam[52], T.Adye[38], P.Adzic[12], Z.Albrecht[18], T.Alderweireld[2], G.D.Alekseev[17], R.Alemany[51], T.Allmendinger[18], P.P.Allport[23], S.Almehed[25], U.Amaldi[9,29], N.Amapane[47], S.Amato[49], E.G.Anassontzis[3], P.Andersson[46], A.Andreazza[9], S.Andringa[22], P.Antilogus[26], W-D.Apel[18], Y.Arnoud[9], B.Åsman[46], J-E.Augustin[26], A.Augustinus[9], P.Baillon[9], A.Ballestrero[47], P.Bambade[20], F.Barao[22], G.Barbiellini[48], R.Barbier[26], D.Y.Bardin[17], G.Barker[18], A.Baroncelli[40], M.Battaglia[16], M.Baubillier[24], K-H.Becks[54], M.Begalli[6], A.Behrmann[54], P.Beilliere[8], Yu.Belokopytov[9], K.Belous[44], N.C.Benekos[33], A.C.Benvenuti[5], C.Berat[15], M.Berggren[24], D.Bertrand[2], M.Besancon[41], M.S.Bilenky[17], M-A.Bizouard[20], D.Bloch[10], H.M.Blom[32], M.Bonesini[29], M.Boonekamp[41], P.S.L.Booth[23], G.Borisov[20], C.Bosio[43], O.Botner[50], E.Boudinov[32], B.Bouquet[20], C.Bourdarios[20], T.J.V.Bowcock[23], I.Boyko[17], I.Bozovic[12], M.Bozzo[14], M.Bracko[45], P.Branchini[40], R.A.Brenner[50], P.Bruckman[9], J-M.Brunet[8], L.Bugge[34], T.Buran[34], B.Buschbeck[52], P.Buschmann[54], S.Cabrera[51], M.Caccia[28], M.Calvi[29], T.Camporesi[9], V.Canale[39], F.Carena[9], L.Carroll[23], C.Caso[14], M.V.Castillo Gimenez[51], A.Cattai[9], F.R.Cavallo[5], V.Chabaud[9], P.Chapkin[44], Ph.Charpentier[9], P.Checchia[37], G.A.Chelkov[17], R.Chierici[47], P.Chliapnikov[9,44], P.Chochula[7], V.Chorowicz[26], J.Chudoba[31], K.Cieslik[19], P.Collins[9], R.Contri[14], E.Cortina[51], G.Cosme[20], F.Cossutti[9], M.Costa[51], H.B.Crawley[1], D.Crennell[38], S.Crepe[15], G.Crosetti[14], J.Cuevas Maestro[35], S.Czellar[16], M.Davenport[9], W.Da Silva[24], G.Della Ricca[48], P.Delpierre[27], N.Demaria[47], A.De Angelis[48], W.De Boer[18], C.De Clercq[2], B.De Lotto[48], A.De Min[37], L.De Paula[49], H.Dijkstra[9], L.Di Ciaccio[9,39], J.Dolbeau[8], K.Doroba[53], M.Dracos[10], J.Drees[54], M.Dris[33], A.Duperrin[26], J-D.Durand[9], G.Eigen[4], T.Ekelof[50], G.Ekspong[46], M.Ellert[50], M.Elsing[9], J-P.Engel[10], M.Espirito Santo[9], G.Fanourakis[12], D.Fassouliotis[12], J.Fayot[24], M.Feindt[18], J.Fernandez[42], A.Ferrer[51], E.Ferrer-Ribas[20], F.Ferro[14], S.Fichet[24], A.Firestone[1], U.Flagmeyer[54], H.Foeth[9], E.Fokitis[33], F.Fontanelli[14], B.Franek[38], A.G.Frodesen[4], R.Fruhwirth[52], F.Fulda-Quenzer[20], J.Fuster[51], A.Galloni[23], D.Gamba[47], S.Gamblin[20], M.Gandelman[49], C.Garcia[51], C.Gaspar[9], M.Gaspar[49], U.Gasparini[37], Ph.Gavillet[9], E.N.Gazis[33], D.Gele[10], T.Geralis[12], N.Ghodbane[26], I.Gil[51], F.Glege[54], R.Gokieli[9,53], B.Golob[9,45], G.Gomez-Ceballos[42], P.Goncalves[22], I.Gonzalez Caballero[42], G.Gopal[38], L.Gorn[1], Yu.Gouz[44], V.Gracco[14], J.Grahl[1], E.Graziani[40], P.Gris[41], G.Grosdidier[20], K.Grzelak[53], J.Guy[38], C.Haag[18], F.Hahn[9], S.Hahn[54], S.Haider[9], A.Hallgren[50], K.Hamacher[54], J.Hansen[34], F.J.Harris[36], F.Hauler[18], V.Hedberg[9,25], S.Heising[18], J.J.Hernandez[51], P.Herquet[2], H.Herr[9], J.-M.Heuser[54], E.Higon[51], S-O.Holmgren[46], P.J.Holt[36], S.Hoorelbeke[2], M.Houlden[23], J.Hrubec[52], M.Huber[18], G.J.Hughes[23], K.Hultqvist[9,46], J.N.Jackson[23], R.Jacobsson[9], P.Jalocha[19], R.Janik[7], Ch.Jarlskog[25], G.Jarlskog[25], P.Jarry[41], B.Jean-Marie[20], D.Jeans[36], E.K.Johansson[46], P.Jonsson[26], C.Joram[9], P.Juillot[10], L.Jungermann[18], F.Kapusta[24], K.Karafasoulis[12], S.Katsanevas[26], E.C.Katsoufis[33], R.Keranen[18], G.Kernel[45], B.P.Kersevan[45], Yu.Khokhlov[44], B.A.Khomenko[17], N.N.Khovanski[17], A.Kiiskinen[16], B.King[23], A.Kinvig[23], N.J.Kjaer[9], O.Klapp[54], H.Klein[9], P.Kluit[32], P.Kokkinias[12], V.Kostioukhine[44], C.Kourkoumelis[3], O.Kouznetsov[17], M.Krammer[52], E.Kriznic[45], Z.Krumstein[17], P.Kubinec[7], J.Kurowska[53], K.Kurvinen[16], J.W.Lamsa[1], D.W.Lane[1], V.Lapin[44], J-P.Laugier[41], R.Lauhakangas[16], G.Leder[52], F.Ledroit[15], V.Lefebure[2], L.Leinonen[46], A.Leisos[12], R.Leitner[31], G.Lenzen[54], V.Lepeltier[20], T.Lesiak[19], M.Lethuillier[41], J.Libby[36], W.Liebig[54], D.Liko[9], A.Lipniacka[9,46], I.Lippi[37], B.Loerstad[25], J.G.Loken[36], J.H.Lopes[49], J.M.Lopez[42], R.Lopez-Fernandez[15], D.Loukas[12], P.Lutz[41], L.Lyons[36], J.MacNaughton[52], J.R.Mahon[6], A.Maio[22], A.Malek[54], T.G.M.Malmgren[46], S.Maltezos[33], V.Malychev[17], F.Mandl[52], J.Marco[42], R.Marco[42], B.Marechal[49], M.Margoni[37], J-C.Marin[9], C.Mariotti[9], A.Markou[12], C.Martinez-Rivero[20], S.Marti i Garcia[9], J.Masik[13], N.Mastroyiannopoulos[12], F.Matorras[42], C.Matteuzzi[29], G.Matthiae[39], F.Mazzucato[37], M.Mazzucato[37], M.Mc Cubbin[23], R.Mc Kay[1], R.Mc Nulty[23], G.Mc Pherson[23], C.Meroni[28], W.T.Meyer[1], A.Miagkov[44], E.Migliore[9], L.Mirabito[26], W.A.Mitaroff[52], U.Mjoernmark[25], T.Moa[46], M.Moch[18], R.Moeller[30], K.Moenig[9,11], M.R.Monge[14], D.Moraes[49], X.Moreau[24], P.Morettini[14], G.Morton[36], U.Mueller[54], K.Muenich[54], M.Mulders[32], C.Mulet-Marquis[15], R.Muresan[25], W.J.Murray[38], B.Muryn[19], G.Myatt[36], T.Myklebust[34], F.Naraghi[15], M.Nassiakou[12], F.L.Navarria[5], K.Nawrocki[53], P.Negri[29], N.Neufeld[9], R.Nicolaidou[41], B.S.Nielsen[30], P.Niezurawski[53], M.Nikolenko[10,17], V.Nomokonov[16], A.Nygren[25], V.Obraztsov[44], A.G.Olshevski[17], A.Onofre[22], R.Orava[16], G.Orazi[10], K.Osterberg[16], A.Ouraou[41], A.Oyanguren[51], M.Paganoni[29], S.Paiano[5], R.Pain[24], R.Paiva[22], J.Palacios[36], H.Palka[19], Th.D.Papadopoulou[9,33], L.Pape[9], C.Parkes[9], F.Parodi[14], U.Parzefall[23], A.Passeri[40], O.Passon[54], T.Pavel[25], M.Pegoraro[37], L.Peralta[22], M.Pernicka[52], A.Perrotta[5], C.Petridou[48], A.Petrolini[14], H.T.Phillips[38], F.Pierre[41], M.Pimenta[22], E.Piotto[28], T.Podobnik[45], M.E.Pol[6], G.Polok[19], P.Poropat[48], V.Pozdniakov[17], P.Privitera[39], N.Pukhaeva[17], A.Pullia[29], D.Radojicic[36], S.Ragazzi[29], H.Rahmani[33], J.Rames[13], P.N.Ratoff[21], A.L.Read[34], P.Rebecchi[9], N.G.Redaelli[29], M.Regler[52], J.Rehn[18], D.Reid[32], P.Reinertsen[4], R.Reinhardt[54], P.B.Renton[36], L.K.Resvanis[3], F.Richard[20], J.Ridky[13], G.Rinaudo[47], I.Ripp-Baudot[10], O.Rohne[34], A.Romero[47], P.Ronchese[37], E.I.Rosenberg[1], P.Rosinsky[7], P.Roudeau[20], T.Rovelli[5], Ch.Royon[41], V.Ruhlmann-Kleider[41], A.Ruiz[42], H.Saarikko[16], Y.Sacquin[41], A.Sadovsky[17], G.Sajot[15], J.Salt[51], D.Sampsonidis[12], M.Sannino[14], A.Savoy-Navarro[24], Ph.Schwemling[24], B.Schwering[54], U.Schwickerath[18], F.Scuri[48], P.Seager[21], Y.Sedykh[17], A.M.Segar[36], N.Seibert[18], R.Sekulin[38], G.Sette[14], R.C.Shellard[6], M.Siebel[54], L.Simard[41], F.Simonetto[37], A.N.Sisakian[17], G.Smadja[26], O.Smirnova[25], G.R.Smith[38], O.Solovianov[44], A.Sopczak[18], R.Sosnowski[53], T.Spassov[22], E.Spiriti[40], S.Squarcia[14], C.Stanescu[40], M.Stanitzki[18], K.Stevenson[36], A.Stocchi[20], J.Strauss[52], R.Strub[10], B.Stugu[4], M.Szczekowski[53], M.Szeptycka[53], T.Tabarelli[29], A.Taffard[23], F.Tegenfeldt[50], F.Terranova[29], J.Timmermans[32], N.Tinti[5], L.G.Tkatchev[17], M.Tobin[23], S.Todorova[9], A.Tomaradze[2], B.Tome[22], A.Tonazzo[9], L.Tortora[40], P.Tortosa[51], G.Transtromer[25], D.Treille[9], G.Tristram[8], M.Trochimczuk[53], C.Troncon[28], M-L.Turluer[41], I.A.Tyapkin[17], P.Tyapkin[25],

S.Tzamarias[12], O.Ullaland[9], V.Uvarov[44], G.Valenti[9,5], E.Vallazza[48], P.Van Dam[32], W.Van den Boeck[2], W.K.Van Doninck[2], J.Van Eldik[9,32], A.Van Lysebetten[2], N.van Remortel[2], I.Van Vulpen[32], G.Vegni[28], L.Ventura[37], W.Venus[38,9], F.Verbeure[2], P.Verdier[26], M.Verlato[37], L.S.Vertogradov[17], V.Verzi[28], D.Vilanova[41], L.Vitale[48], E.Vlasov[44], A.S.Vodopyanov[17], G.Voulgaris[3], V.Vrba[13], H.Wahlen[54], C.Walck[46], A.J.Washbrook[23], C.Weiser[9], D.Wicke[9], J.H.Wickens[2], G.R.Wilkinson[36], M.Winter[10], M.Witek[19], G.Wolf[9], J.Yi[1], O.Yushchenko[44], A.Zalewska[19], P.Zalewski[53], D.Zavrtanik[45], E.Zevgolatakos[12], N.I.Zimin[17,25], A.Zintchenko[17], Ph.Zoller[10], G.C.Zucchelli[46], G.Zumerle[37]

[1] Department of Physics and Astronomy, Iowa State University, Ames IA 50011-3160, USA
[2] Physics Department, Univ. Instelling Antwerpen, Universiteitsplein 1, B-2610 Antwerpen, Belgium
and IIHE, ULB-VUB, Pleinlaan 2, B-1050 Brussels, Belgium
and Faculté des Sciences, Univ. de l'Etat Mons, Av. Maistriau 19, B-7000 Mons, Belgium
[3] Physics Laboratory, University of Athens, Solonos Str. 104, GR-10680 Athens, Greece
[4] Department of Physics, University of Bergen, Allégaten 55, NO-5007 Bergen, Norway
[5] Dipartimento di Fisica, Università di Bologna and INFN, Via Irnerio 46, IT-40126 Bologna, Italy
[6] Centro Brasileiro de Pesquisas Físicas, rua Xavier Sigaud 150, BR-22290 Rio de Janeiro, Brazil
and Depto. de Física, Pont. Univ. Católica, C.P. 38071 BR-22453 Rio de Janeiro, Brazil
and Inst. de Física, Univ. Estadual do Rio de Janeiro, rua São Francisco Xavier 524, Rio de Janeiro, Brazil
[7] Comenius University, Faculty of Mathematics and Physics, Mlynska Dolina, SK-84215 Bratislava, Slovakia
[8] Collège de France, Lab. de Physique Corpusculaire, IN2P3-CNRS, FR-75231 Paris Cedex 05, France
[9] CERN, CH-1211 Geneva 23, Switzerland
[10] Institut de Recherches Subatomiques, IN2P3 - CNRS/ULP - BP20, FR-67037 Strasbourg Cedex, France
[11] Now at DESY-Zeuthen, Platanenallee 6, D-15735 Zeuthen, Germany
[12] Institute of Nuclear Physics, N.C.S.R. Demokritos, P.O. Box 60228, GR-15310 Athens, Greece
[13] FZU, Inst. of Phys. of the C.A.S. High Energy Physics Division, Na Slovance 2, CZ-180 40, Praha 8, Czech Republic
[14] Dipartimento di Fisica, Università di Genova and INFN, Via Dodecaneso 33, IT-16146 Genova, Italy
[15] Institut des Sciences Nucléaires, IN2P3-CNRS, Université de Grenoble 1, FR-38026 Grenoble Cedex, France
[16] Helsinki Institute of Physics, HIP, P.O. Box 9, FI-00014 Helsinki, Finland
[17] Joint Institute for Nuclear Research, Dubna, Head Post Office, P.O. Box 79, RU-101 000 Moscow, Russian Federation
[18] Institut für Experimentelle Kernphysik, Universität Karlsruhe, Postfach 6980, DE-76128 Karlsruhe, Germany
[19] Institute of Nuclear Physics and University of Mining and Metalurgy, Ul. Kawiory 26a, PL-30055 Krakow, Poland
[20] Université de Paris-Sud, Lab. de l'Accélérateur Linéaire, IN2P3-CNRS, Bât. 200, FR-91405 Orsay Cedex, France
[21] School of Physics and Chemistry, University of Lancaster, Lancaster LA1 4YB, UK
[22] LIP, IST, FCUL - Av. Elias Garcia, 14-1°, PT-1000 Lisboa Codex, Portugal
[23] Department of Physics, University of Liverpool, P.O. Box 147, Liverpool L69 3BX, UK
[24] LPNHE, IN2P3-CNRS, Univ. Paris VI et VII, Tour 33 (RdC), 4 place Jussieu, FR-75252 Paris Cedex 05, France
[25] Department of Physics, University of Lund, Sölvegatan 14, SE-223 63 Lund, Sweden
[26] Université Claude Bernard de Lyon, IPNL, IN2P3-CNRS, FR-69622 Villeurbanne Cedex, France
[27] Univ. d'Aix - Marseille II - CPP, IN2P3-CNRS, FR-13288 Marseille Cedex 09, France
[28] Dipartimento di Fisica, Università di Milano and INFN-MILANO, Via Celoria 16, IT-20133 Milan, Italy
[29] Dipartimento di Fisica, Univ. di Milano-Bicocca and INFN-MILANO, Piazza delle Scienze 2, IT-20126 Milan, Italy
[30] Niels Bohr Institute, Blegdamsvej 17, DK-2100 Copenhagen Ø, Denmark
[31] IPNP of MFF, Charles Univ., Areal MFF, V Holesovickach 2, CZ-180 00, Praha 8, Czech Republic
[32] NIKHEF, Postbus 41882, NL-1009 DB Amsterdam, The Netherlands
[33] National Technical University, Physics Department, Zografou Campus, GR-15773 Athens, Greece
[34] Physics Department, University of Oslo, Blindern, NO-1000 Oslo 3, Norway
[35] Dpto. Fisica, Univ. Oviedo, Avda. Calvo Sotelo s/n, ES-33007 Oviedo, Spain
[36] Department of Physics, University of Oxford, Keble Road, Oxford OX1 3RH, UK
[37] Dipartimento di Fisica, Università di Padova and INFN, Via Marzolo 8, IT-35131 Padua, Italy
[38] Rutherford Appleton Laboratory, Chilton, Didcot OX11 OQX, UK
[39] Dipartimento di Fisica, Università di Roma II and INFN, Tor Vergata, IT-00173 Rome, Italy
[40] Dipartimento di Fisica, Università di Roma III and INFN, Via della Vasca Navale 84, IT-00146 Rome, Italy
[41] DAPNIA/Service de Physique des Particules, CEA-Saclay, FR-91191 Gif-sur-Yvette Cedex, France
[42] Instituto de Fisica de Cantabria (CSIC-UC), Avda. los Castros s/n, ES-39006 Santander, Spain
[43] Dipartimento di Fisica, Università degli Studi di Roma La Sapienza, Piazzale Aldo Moro 2, IT-00185 Rome, Italy
[44] Inst. for High Energy Physics, Serpukov P.O. Box 35, Protvino, (Moscow Region), Russian Federation
[45] J. Stefan Institute, Jamova 39, SI-1000 Ljubljana, Slovenia and Laboratory for Astroparticle Physics,
Nova Gorica Polytechnic, Kostanjeviska 16a, SI-5000 Nova Gorica, Slovenia,
and Department of Physics, University of Ljubljana, SI-1000 Ljubljana, Slovenia
[46] Fysikum, Stockholm University, Box 6730, SE-113 85 Stockholm, Sweden
[47] Dipartimento di Fisica Sperimentale, Università di Torino and INFN, Via P. Giuria 1, IT-10125 Turin, Italy
[48] Dipartimento di Fisica, Università di Trieste and INFN, Via A. Valerio 2, IT-34127 Trieste, Italy
and Istituto di Fisica, Università di Udine, IT-33100 Udine, Italy
[49] Univ. Federal do Rio de Janeiro, C.P. 68528 Cidade Univ., Ilha do Fundão BR-21945-970 Rio de Janeiro, Brazil
[50] Department of Radiation Sciences, University of Uppsala, P.O. Box 535, SE-751 21 Uppsala, Sweden
[51] IFIC, Valencia-CSIC, and D.F.A.M.N., U. de Valencia, Avda. Dr. Moliner 50, ES-46100 Burjassot (Valencia), Spain
[52] Institut für Hochenergiephysik, Österr. Akad. d. Wissensch., Nikolsdorfergasse 18, AT-1050 Vienna, Austria
[53] Inst. Nuclear Studies and University of Warsaw, Ul. Hoza 69, PL-00681 Warsaw, Poland
[54] Fachbereich Physik, University of Wuppertal, Postfach 100 127, DE-42097 Wuppertal, Germany

1 Introduction

The cross-section for the doubly resonant production of W bosons has been measured with the data sample collected by DELPHI at the average centre-of-mass energy of 188.63 ± 0.04 GeV. Depending on the decay mode of each W boson, fully hadronic, mixed hadronic-leptonic ("semileptonic") or fully leptonic final states were obtained, for which the Standard Model branching fractions are 45.6%, 43.9% and 10.5%, respectively. The detector was essentially unchanged compared to previous years and detailed descriptions of the DELPHI apparatus and its performance can be found in [1,2]. The luminosity was measured using the Small Angle Tile Calorimeter [3]. The total integrated luminosity corresponds to 155 pb^{-1}; its systematic error is estimated to be $\pm 0.6\%$, which is dominated by the experimental uncertainty on the Bhabha measurements of $\pm 0.5\%$. The luminosities used for the different selections correspond to those data for which all elements of the detector essential to each specific analysis were fully functional. The criteria for the selection of WW events are reviewed in section 2. Generally they follow those used for the cross-section measurements at lower centre-of-mass energies [4–6], but for the 4-jet final state a more efficient selection has been applied using a neural network, and the selection of leptons has been modified to improve the efficiency for τ leptons. In section 3 the total cross-section and the branching fractions of the W boson are presented.

The cross-sections determined in this analysis correspond to W pair production through the three doubly resonant tree-level diagrams ("CC03 diagrams" [7]) involving s-channel γ and Z exchange and t-channel ν exchange. The selection efficiencies were defined with respect to these diagrams only and were determined using the full simulation program DELSIM [8] with the PYTHIA 5.7 event generator [9]. In addition to the production via the CC03 diagrams, the four-fermion final states corresponding to some decay modes may be produced via other Standard Model diagrams involving either zero, one, or two massive vector bosons. Corrections which account for the interference between the CC03 diagrams and the additional diagrams are generally expected to be negligible at this energy, except for final states with electrons or positrons. In these cases correction factors were determined from simulation using the 4-fermion generator EXCALIBUR [10] and were found to be consistent with unity within an uncertainty of $\pm 2\%$.

2 Event selection and cross-sections

2.1 Fully hadronic final state

A feed-forward neural network (see e.g. [11,12]) was used to improve the selection quality of $W^+W^- \to q\overline{q}q\overline{q}$ from 2-fermion (mainly $Z/\gamma \to q\overline{q}$) and 4-fermion background (mainly $ZZ \to q\bar{q}x\bar{x}$). Compared to an analysis based on sequential cuts [6], the selection efficiency for the signal was increased by about 10% for the same purity. The network is based on the JETNET package [13], uses the standard back-propagation algorithm, and consists of three layers with 13 input nodes, 7 hidden nodes and one output node.

A preselection of the events was performed with the following criteria:

- a reconstructed effective centre-of-mass energy [14] $\sqrt{s'} > 115$ GeV;
- 4 or more reconstructed jets when clustering with LUCLUS [15] at $d_{join} = 4.0\ \mathrm{GeV}/c$;
- total particle multiplicity ≥ 3 for each jet.

Each event was forced into a 4-jet configuration. The following jet and event observables were chosen as input variables, taking into account previous neural network studies to optimize input variables for the WW and 2-fermion separation [16]:

1. the difference between the maximum and minimum jet energy after a 4C fit, imposing 4-momentum conservation on the event;
2. the minimum angle between two jets after the 4C fit;
3. the value of d_{join} from the cluster algorithm LUCLUS for the migration of 4 jets into 3 jets;
4. the minimum particle multiplicity of all jets;
5. the reconstructed effective centre-of-mass energy $\sqrt{s'}$;
6. the maximum probability (for all possible jet pairings) for a 2C fit (two objects with W-mass);
7. thrust;
8. sphericity;
9. the mean rapidity of all particles with respect to the thrust axis;
10. the sum of the cubes of the magnitudes of the momenta of the 7 highest momentum particles $\sum_{i=1}^{7} |\vec{p}_i|^3$;
11. the minimum jet broadening B_{min} [17];
12. the Fox-Wolfram-moment H3 [18];
13. the Fox-Wolfram-moment H4.

The training of the neural network was performed with 3500 signal events ($WW \to q\bar{q}q\bar{q}$) and 3500 $Z/\gamma \to q\bar{q}$ background events simulated with the PYTHIA 5.7 event generator. Afterwards the network output was calculated for other independent samples of simulated WW, Z/γ and ZZ events and for the real data. Figure 1 shows the distribution of the neural network output for data and simulated events.

For each bin the fractional efficiencies of the selection of WW decays and the background contributions were estimated from simulation. Events were finally retained if the neural network output variable was larger than -0.5. The resulting selection efficiencies for the WW channels are listed in the second column of Table 1 together with the estimated backgrounds.

	efficiencies for selected channels			
channel	$jjjj$	$jje\nu$	$jj\mu\nu$	$jj\tau\nu$
$q\bar{q}q\bar{q}$	**0.887**	0.	0.	0.018
$q\bar{q}e\nu$	0.009	**0.661**	0.	0.115
$q\bar{q}\mu\nu$	0.004	0.	**0.865**	0.056
$q\bar{q}\tau\nu$	0.028	0.039	0.034	**0.491**
background (pb)	1.788	0.159	0.075	0.437
selected events	1298	259	328	324
luminosity (pb^{-1})	154.35	153.94		

Table 1: Selection efficiencies, background and data for the hadronic and semileptonic final states.

A relative uncertainty on the efficiency of $\pm 0.6\%$ was estimated from the following studies:

- Comparison of the simulation with real data, which were taken at a centre-of-mass energy of 91.2 GeV with the same detector and trigger configuration and analysed

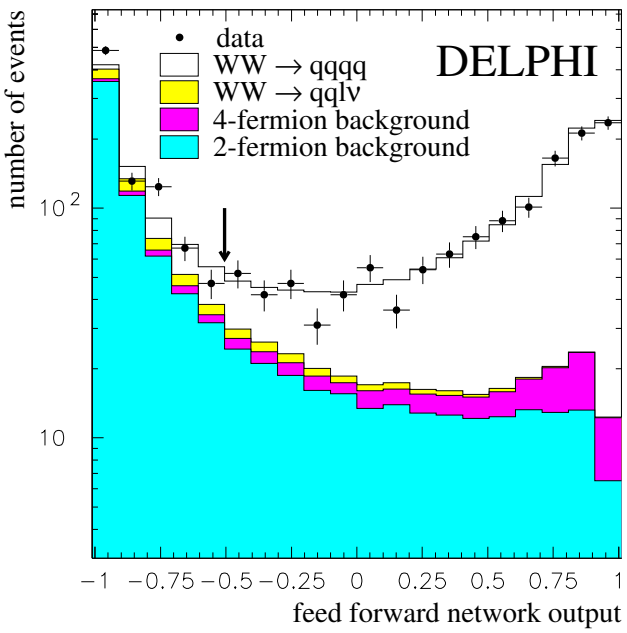

Figure 1: Distribution of the neural network output variable for 4-jet events. The points show the data and the histograms are the predicted distributions for signal and background. Events to the right of the vertical arrow were accepted for the event sample.

with the same reconstruction software as the 189 GeV data. For this comparison, the technique of mixing Lorentz-boosted Z events was used, which transformed two independent hadronic Z decays into a pseudo W pair event by applying an appropriate boost to the particles of each Z decay. In this study a difference of 0.17% was observed.

- Variation of the efficiency using different hadronization models (JETSET 7.4 [9] and ARIADNE [19]) giving 0.59%. Within this error variations of the efficiency from different modelling of Bose-Einstein correlations in the generator were found to be negligable; this is also expected for final state interactions between quarks from different W bosons ("Colour Reconnection").

The cross-section for the expected total background was estimated from the simulations to be (1.79 ± 0.09) pb. The main contribution (1.42 pb) comes from $q\bar{q}(\gamma)$ events with gluon radiation, the rest from non-WW 4-fermion final states. The systematic uncertainty on the background was estimated from the variation of the selection efficiencies for the different backgrounds when different hadronization models were used (JETSET 7.4 and ARIADNE). A total uncertainty of $\pm 5\%$ was estimated from this variation (4.5%) and from differences between data and simulation due to imperfections of the generator models. Furthermore, the influences of the different parameters of the neural network structure, its learning algorithm, and of the preselection have been investigated and found to be negligible.

A total of 1298 events were selected in the data sample. The cross-section for fully hadronic events was obtained from a binned maximum likelihood fit to the distribution

of the neural network output variable above -0.5, taking into account the expected background in each bin. The result is

$$\sigma_{WW}^{qqqq} = \sigma_{WW}^{tot} \times \mathrm{BR}(WW \to q\bar{q}q\bar{q}) = 7.36 \pm 0.26 \text{ (stat)} \pm 0.10 \text{ (syst)} \text{ pb},$$

where $\mathrm{BR}(WW \to q\bar{q}q\bar{q})$ is the probability for the WW pair to give a purely hadronic final state. The first error is statistical and the second is systematic. The systematic error includes contributions from the uncertainties on efficiency and background, and on the luminosity.

2.2 Semileptonic final state

Events in which one of the W bosons decays into $l\nu$ and the other one into quarks are characterized by two hadronic jets, one isolated lepton (coming either directly from the W decay or from the cascade decay $W \to \tau\nu \to e\nu\nu\nu$ or $\mu\nu\nu\nu$) or a low multiplicity jet due to a τ decay, and missing momentum resulting from the neutrino. The major background comes from $q\bar{q}(\gamma)$ production and from four-fermion final states containing two quarks and two leptons of the same flavour.

Events were required to show hadronic activity (at least 6 charged particles), to have a total visible energy of at least 50 GeV and to be compatible with a 3-jet topology on application of the LUCLUS [15] clustering algorithm with a value of d_{join} between 2 and 20 GeV/c. A lepton had to be found in the event according to one of the following criteria:

- a single charged particle identified as described in [5] as an electron or a muon, and with at least 5 GeV of energy;
- a single charged particle of momentum, p, above 5 GeV/c, not identified as a lepton, but isolated from other particles by $p \cdot \theta_{iso} > 100$ GeV/c·degrees, where θ_{iso} is the angle formed with the closest charged particle with a momentum of at least 1 GeV/c;
- a low multiplicity jet (with less than 4 charged particles) with an energy above 5 GeV, polar angle of its axis with respect to the beam axis between 20° and 160°, and with at least 15% of its energy carried by charged particles.

When several candidate leptons with the same flavour were found in the event, the one with highest $p \cdot \theta_{iso}$ (single-track case) or smallest opening angle (jet case) was chosen. Tests on WW simulation show that the correct lepton was chosen in more than 99% of the ambiguous events.

Events not compatible with a 3-jet topology or with the lepton too close to fragmentation products or inside a hadronic jet were recovered by looking for particles inside jets with energy above 30 GeV and identified as electrons or muons. In this case additional cuts were imposed on the impact parameter of the lepton with respect to the beam spot and on the angles which the missing momentum formed with respect to the beam direction and the lepton itself.

The background contribution arising from the radiative return to the Z peak was highly suppressed by rejecting events with the direction of the missing momentum close to the beam axis or with a detected photon with an energy above 50 GeV. The cut on the polar angle of the missing momentum was tighter for $q\bar{q}\tau\nu$ candidate events. The four-fermion neutral current background ($q\bar{q}l\bar{l}$) was suppressed by rejecting those events in which a second isolated and energetic lepton of the same flavour as the main candidate was found. Non-resonant contributions to the $q\bar{q}l\nu$ final state were reduced by requiring

the invariant mass of the hadronic system to be larger than 20 GeV/c^2 and of the lepton-missing momentum system to be larger than 10 GeV/c^2.

The different leptonic decays were classified in the following way:

- $WW \to q\bar{q}\mu\nu$
  The lepton was identified as a muon. The contamination from $q\bar{q}\tau\nu$ with $\tau \to \mu\nu\nu$ was suppressed by requiring that, if the muon momentum was below 45 GeV/c, either the missing mass in the event was below 55 GeV/c^2, or the fitted mass from a 2C kinematic fit with both W bosons constrained to have the same mass was above 75 GeV/c^2.
- $WW \to q\bar{q}e\nu$
  The lepton was identified as an electron. A cut on the aplanarity of the event, defined as the angle between the lepton direction and the plane of the two jets, was applied in order to reduce radiative and non-radiative QCD background. The contribution from the process $ee \to Zee$ was reduced by imposing requirements on the invariant mass of the electron and the missing momentum (assumed to be a single electron in the beam pipe). A procedure identical to that just described for the muon channel was then applied to reduce the contamination of $q\bar{q}\tau\nu$ events.
- $WW \to q\bar{q}\tau\nu$
  The event was not classified as an electron or a muon decay. In order to suppress the background from e^+e^- annihilations into $q\bar{q}(\gamma)$, events containing a 1-prong candidate τ had to have aplanarity above 20°. For multi-prong τ events a cut on the effective centre-of-mass energy $\sqrt{s'}$ was added, requiring it to be between 105 and 175 GeV. In both cases the hadronic system was rescaled to the beam energy and cuts were applied to reject very low (less than 15 GeV/c^2) and very high (more than 90 GeV/c^2) invariant masses in the resulting jet-jet system or lepton-missing momentum system.

Figure 2 shows the distribution of the momentum of the selected leptons compared with the expectations from the simulation of signal and backgrounds. The numbers of selected events, efficiencies and backgrounds for each lepton flavour are shown in Table 1. The efficiencies include corrections to account for an imperfect description of the misidentification of electrons or muons as taus in the simulation, for which an uncertainty of 1.0% for electrons and 0.6% for muons has been taken into account in the determination of the W branching ratios. The overall efficiency of the selection of $WW \to q\bar{q}l\nu$ events was estimated to be (75.4 $\pm$ 0.7)%, varying significantly with lepton type: 92% for μ, 78% for e and 56% for τ (see Table 1). The total expected background was estimated to be (671 $\pm$ 40) fb. The errors on efficiency and background include all systematic uncertainties.

A total of 911 events were selected as semileptonic W decays; the number of events observed in the different lepton channels was found to be consistent with lepton universality. With the values given in Table 1 for selected events, efficiencies and backgrounds, and assuming lepton universality, a likelihood fit yields a cross-section:

$$\sigma_{WW}^{l\nu qq} = \sigma_{WW}^{tot} \times BR(WW \to l\nu q\bar{q}) = 6.77 \pm 0.26(\text{stat}) \pm 0.12(\text{syst}) \text{ pb}.$$

The systematic error includes contributions from efficiency and background, four-fermion interference in the electron channel, imperfect track reconstruction description in the simulation and uncertainty in the luminosity measurement.

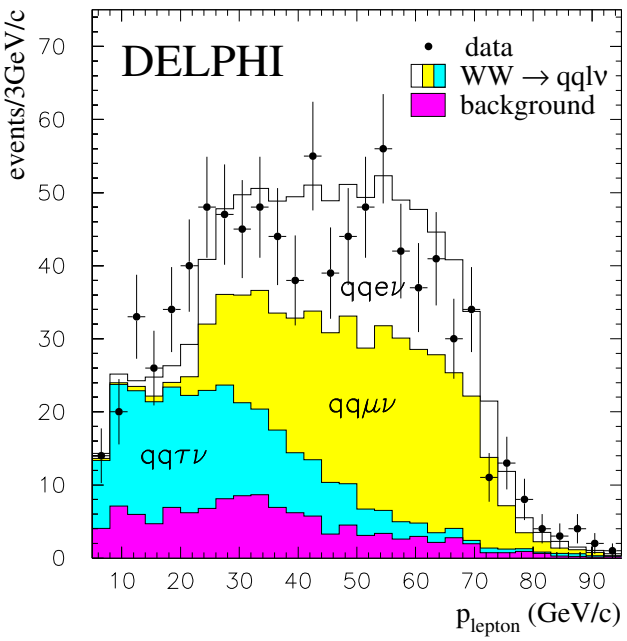

Figure 2: Distribution of the lepton momentum for semileptonic events. The points show the data and the histograms are the predicted distributions for signal and background. The latter includes small contributions from other WW channels.

2.3 Fully leptonic final state

Events in which both W bosons decay into $l\nu$ are characterized by low multiplicity, a clean two-jet topology with two energetic, acollinear and acoplanar leptons of opposite charge, and with large missing momentum and energy. The relevant backgrounds are di-leptons from $e^+e^- \to Z(\gamma)$, Bhabha scattering, two-photon collisions, Ze^+e^-, ZZ and single W events.

The selection was performed in three steps. First a leptonic preselection was made followed by $\mu/e/\tau$ identification in both jets. Finally different cuts were applied for each channel to reject the remaining background, which was different in each case.

The leptonic preselection aimed to select a sample enriched in leptonic events. All particles in the event were clustered into jets using the LUCLUS algorithm [15] (d_{join} = 6.5 GeV/c) and only events with two reconstructed jets, containing at least one charged particle each, were retained. A charged particle multiplicity between 2 and 6 was required and at least one jet had to have only one charged particle. The leading particle (that with the largest momentum) in each jet was required to have polar angle $|\cos\theta_l| < 0.98$. In order to reduce the background from two-photon collisions and radiative di-lepton events, the event acoplanarity, θ_{acop}, defined as the acollinearity of the two jet directions projected onto the plane perpendicular to the beam axis, had to be above 5°. In addition, the total momentum transverse to the beam direction, P_t, had to exceed 4% of the centre-of-mass energy $\sqrt{s}$. The associated electromagnetic energy for both leading particles was required to be less than $0.4 \cdot \sqrt{s}$ to reject Bhabha scattering.

For this sample each particle was identified as μ, e or hadron. Slightly different criteria for lepton identification were applied, depending on whether the particle was in the barrel

region ($43^\circ < \theta < 137^\circ$), in the forward region ($\theta < 37^\circ$ or $\theta > 143^\circ$), or in between. A particle was identified as a muon if at least one hit in the muon chambers was associated to it, or if it had deposited energy in the outermost layer of the hadron calorimeter; in addition the energy deposited in the other layers had to be compatible with that from a minimum ionizing particle. For the identification of a particle as an electron the energies deposited in the electromagnetic calorimeters, in the different layers of the hadron calorimeter, and in addition the energy loss in the time projection chamber were used. A lepton was identified as a cascade decay from $W \to \tau\nu_\tau$ if the momentum was lower than 20 GeV/c.

After the preselection and the channel identification, different cuts were applied depending on the channel in order to reject the remaining background. For all channels except $WW \to \mu\nu\mu\nu$, the visible energy of the particles with $|\cos\theta| < 0.9$ had to exceed $0.06 \cdot \sqrt{s}$. For all channels with at least one W decaying into $\tau\nu$, the invariant mass of each jet had to be below 3 GeV/c^2, the momentum of the leading particle of a candidate τ jet below $0.4 \cdot \sqrt{s}$, and θ_{acop} above 9°. In addition the following criteria were required for the individual channels:

- $WW \to e\nu e\nu$
  The most important background comes from radiative Bhabha scattering. Therefore a cut on the neutral energy was imposed, and the acoplanarity had to be greater than 7°. In addition a minimum transverse energy was required and the momenta of both leading particles had to be less than 45% of the centre-of-mass energy.
- $WW \to \mu\nu\mu\nu$
  In order to reject radiative di-muon events, the transverse energy was required to satisfy $0.2 \cdot \sqrt{s} < E_t < 0.8 \cdot \sqrt{s}$, and the neutral energy had to be less than 2 GeV.
- $WW \to \tau\nu\tau\nu$
  In order to reduce remaining background from $Z(\gamma)$-decays and from $\gamma\gamma \to \ell\ell$ processes, tighter cuts were applied on the acoplanarity, the transverse momentum and the total transverse energy of the jets. Finally the acollinearity was required to be between 10° and 150°.
- $WW \to e\nu\mu\nu$
  The neutral energy was required to be less than 20 GeV.
- $WW \to \tau\nu e\nu$
  A minimum transverse energy was required. If one of the leading particles was not in the barrel region, additional cuts on the momentum of each leading particle and on the acollinearity were applied to reduce the background from two-photon collisions.
- $WW \to \tau\nu\mu\nu$
  The acoplanarity was required to be greater than 11° if at least one leading particle was outside the barrel region.

The distribution of the acoplanarity angle, after having applied all cuts except the one on the acoplanarity, is shown in Figure 3. The numbers of selected events, efficiencies and backgrounds in each channel are shown in Table 2. The overall $l\nu l\nu$ efficiency was (62.9 ± 1.6) %. The efficiencies have been corrected to account for an imperfect simulation of the misidentification of electrons and muons as tau leptons in a similar way as for the semileptonic channel, and the uncertainty in the track reconstruction efficiency is taken into account in the total systematic error. Inefficiencies of the trigger are estimated to be $\leq 0.1\%$. The residual background from non-W and single-W events is 0.134 ± 0.032 pb, where the error includes all systematic effects introduced by the selection criteria.

A total of 183 events were selected in the data sample; the number of events observed in the different di-lepton channels was found to be consistent with lepton universality.

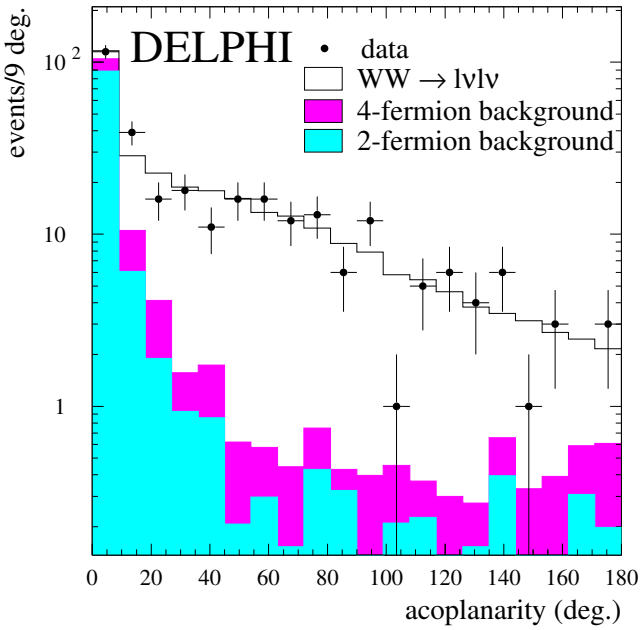

Figure 3: Distribution of the acoplanarity angle for fully-leptonic events. The points show the data and the histograms are the predicted distributions for signal and background.

With the values given in Table 2 for the selected events, efficiencies and backgrounds, and assuming lepton universality, a likelihood fit yields a cross-section

$$\sigma_{WW}^{\ell\nu\ell\nu} = \sigma_{WW}^{tot} \times \mathrm{BR}(WW \to \ell\nu\ell\nu) = 1.68 \pm 0.14\ (\mathrm{stat}) \pm 0.07\ (\mathrm{syst})\ \ \mathrm{pb}.$$

The systematic error has contributions from the efficiency and background determination, four-fermion interferences in the final states with electrons and from the measurement of the luminosity.

	efficiencies for selected channels					
channel	$\tau\nu\tau\nu$	$\tau\nu e\nu$	$\tau\nu\mu\nu$	$e\nu e\nu$	$e\nu\mu\nu$	$\mu\nu\mu\nu$
$\tau\nu\tau\nu$	**0.252**	0.069	0.083	0.005	0.008	0.003
$\tau\nu e\nu$	0.040	**0.433**	0.012	0.044	0.057	0.
$\tau\nu\mu\nu$	0.019	0.008	**0.540**	0.0	0.043	0.047
$e\nu e\nu$	0.005	0.114	0.	**0.474**	0.	0.
$e\nu\mu\nu$	0.004	0.038	0.090	0.001	**0.589**	0.
$\mu\nu\mu\nu$	0.001	0.	0.058	0.	0.002	**0.655**
background (pb)	0.020	0.038	0.026	0.030	0.006	0.014
selected events	15	40	43	20	38	27
luminosity (pb^{-1})	153.81					

Table 2: Selection efficiencies, background and data for the fully leptonic final states.

3 Determination of total cross-section and branching fractions

The total cross-section for WW production and the W leptonic branching fractions were obtained from likelihood fits to the numbers of events observed in each final state. The input numbers are those given in Tables 1 and 2, except for the fully hadronic final state where the binned distribution of the neural network output was used.

From all the final states combined, the leptonic branching fractions with their correlation matrix were obtained as shown in Table 3. They are consistent with lepton universality. The fit was repeated assuming lepton universality, and the results for the leptonic and derived hadronic branching fraction are also given in Table 3. The hadronic branching fraction is in agreement with the Standard Model prediction of 0.675.

Assuming the other parameters of the Standard Model, i.e. elements $|V_{ud}|$, $|V_{us}|$, $|V_{ub}|$, $|V_{cd}|$ and $|V_{cb}|$ of the CKM matrix, lepton couplings to W bosons, and the strong coupling constant α_S, to be fixed at the values given in [20], the measured hadronic branching fraction can be converted [21] into

$$|V_{cs}| = 1.001 \pm 0.040 \text{ (stat)} \pm 0.020 \text{ (syst)},$$

where the uncertainties of the Standard Model parameters are included in the systematic error.

The total cross-section for WW production, with the assumption of Standard Model values for all branching fractions, was found to be

$$\sigma_{WW}^{tot} = 15.83 \pm 0.38 \text{ (stat)} \pm 0.20 \text{ (syst)} \text{ pb}.$$

This result is shown in figure 4 together with the measurements at lower centre-of-mass energies [4–6], and with the Standard Model prediction using GENTLE [22].

The measurement of the branching fractions can be improved by combining the present measurement with those at lower centre-of-mass energies [4–6]. These results, obtained conservatively assuming full correlation of systematics between different energies, are summarized in Table 4.

4 Summary

From a data sample of 155 pb^{-1} integrated luminosity, collected by DELPHI in e^+e^-collisions at a centre-of-mass energy of 188.63 GeV, the individual leptonic branching fractions were found to be in agreement with lepton universality and the W hadronic branching fraction was measured to be

$$\text{BR}(W \to q\bar{q}) = 0.680 \pm 0.008(\text{stat}) \pm 0.004(\text{syst}),$$

in agreement with the Standard Model prediction of 0.675 and compatible with measurements at lower energies by other LEP experiments [23–25]. The total cross-section for the doubly resonant WW process was measured to be

$$\sigma_{WW}^{tot} = 15.83 \pm 0.38(\text{stat}) \pm 0.20(\text{syst}) \text{ pb},$$

assuming Standard Model branching fractions.

channel	branching fraction	stat. error	syst. error	syst. from QCD bkg
$W \to e\nu$	0.1019	0.0064	0.0025	0.0005
$W \to \mu\nu$	0.1076	0.0056	0.0012	0.0005
$W \to \tau\nu$	0.1109	0.0087	0.0031	0.0003

Correlations	$W \to e\nu$	$W \to \mu\nu$	$W \to \tau\nu$
$W \to e\nu$	1.00	-0.02	-0.39
$W \to \mu\nu$	-0.02	1.00	-0.29
$W \to \tau\nu$	-0.39	-0.29	1.00

	assuming lepton universality			
channel	branching fraction	stat. error	syst. error	syst. from QCD bkg
$W \to \ell\nu$	0.1066	0.0028	0.0013	0.0004
$W \to$ hadrons	0.6803	0.0084	0.0040	0.0013

Table 3: W branching fractions from 189 GeV data and correlation matrix for the leptonic branching fractions. The uncertainty from the QCD background (column 5) is included in the systematic error (column 4).

channel	branching fraction	stat. error	syst. error	syst. from QCD bkg
$W \to e\nu$	0.1018	0.0054	0.0026	0.0005
$W \to \mu\nu$	0.1092	0.0048	0.0012	0.0006
$W \to \tau\nu$	0.1105	0.0075	0.0032	0.0004

Correlations	$W \to e\nu$	$W \to \mu\nu$	$W \to \tau\nu$
$W \to e\nu$	1.00	-0.02	-0.38
$W \to \mu\nu$	-0.02	1.00	-0.30
$W \to \tau\nu$	-0.38	-0.30	1.00

	assuming lepton universality			
channel	branching fraction	stat. error	syst. error	syst. from QCD bkg
$W \to \ell\nu$	0.1071	0.0024	0.0014	0.0005
$W \to$ hadrons	0.6789	0.0073	0.0043	0.0015

Table 4: W branching fractions from the combined 161, 172, 183 and 189 GeV data and correlation matrix for the leptonic branching fractions. The uncertainty from the QCD background (column 5) is included in the systematic error (column 4).

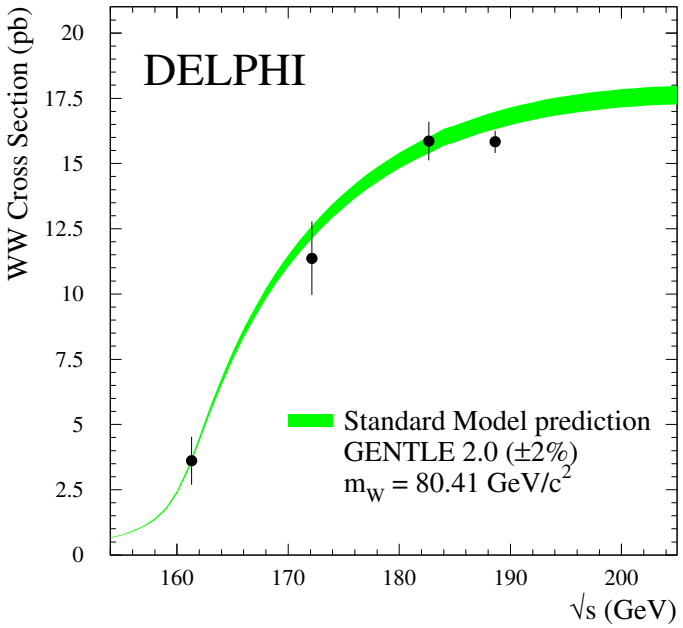

Figure 4: Measurements of the W^+W^- cross-section compared with the Standard Model prediction using [22] and $m_W = 80.41$ GeV/c^2 [20] with a possible uncertainty of $\pm 2\%$ on the computation.

Acknowledgements

We are greatly indebted to our technical collaborators, to the members of the CERN-SL Division for the excellent performance of the LEP collider, and to the funding agencies for their support in building and operating the DELPHI detector.
We acknowledge in particular the support of
Austrian Federal Ministry of Science and Traffics, GZ 616.364/2-III/2a/98,
FNRS–FWO, Belgium,
FINEP, CNPq, CAPES, FUJB and FAPERJ, Brazil,
Czech Ministry of Industry and Trade, GA CR 202/96/0450 and GA AVCR A1010521,
Danish Natural Research Council,
Commission of the European Communities (DG XII),
Direction des Sciences de la Matière, CEA, France,
Bundesministerium für Bildung, Wissenschaft, Forschung und Technologie, Germany,
General Secretariat for Research and Technology, Greece,
National Science Foundation (NWO) and Foundation for Research on Matter (FOM), The Netherlands,
Norwegian Research Council,
State Committee for Scientific Research, Poland, 2P03B06015, 2P03B1116 and SPUB/P03/178/98,
JNICT–Junta Nacional de Investigação Científica e Tecnológica, Portugal,
Vedecka grantova agentura MS SR, Slovakia, Nr. 95/5195/134,
Ministry of Science and Technology of the Republic of Slovenia,
CICYT, Spain, AEN96–1661 and AEN96-1681,

The Swedish Natural Science Research Council,
Particle Physics and Astronomy Research Council, UK,
Department of Energy, USA, DE–FG02–94ER40817.

References

[1] DELPHI Collaboration, P. Aarnio et al., Nucl. Instr. & Meth. **A303** (1991) 233.
[2] DELPHI Collaboration, P. Abreu et al., Nucl. Instr. & Meth. **A378** (1996) 57.
[3] S. J. Alvsvaag et al., Nucl. Instr. & Meth. **A425** (1999) 106.
[4] DELPHI Collaboration, P.Abreu et al., Phys.Lett. **B397** (1997) 158.
[5] DELPHI Collaboration, P.Abreu et al., E. Phys. J. **C2** (1998) 581.
[6] DELPHI Collaboration, P.Abreu et al., Phys. Lett. **B456** (1999) 310.
[7] W. Beenakker et al., *WW cross-sections and distributions*, Physics at LEP2, eds. G. Altarelli, T. Sjöstrand and F. Zwirner, CERN 96-01 (1996) Vol 1, 79.
[8] DELPHI Collaboration: *DELPHI event generation and detector simulation - User Guide*, DELPHI Note 89-67 (1989), unpublished.
[9] T. Sjöstrand, *PYTHIA 5.719 / JETSET 7.4*, Physics at LEP2, eds. G. Altarelli, T. Sjöstrand and F. Zwirner, CERN 96-01 (1996) Vol 2, 41.
[10] F. A. Berends, R. Kleiss and R. Pittau, *EXCALIBUR*, Physics at LEP2, eds. G. Altarelli, T. Sjöstrand and F. Zwirner, CERN 96-01 (1996) Vol 2, 23.
[11] R. Rojas, *Neural Networks - A Systematic Introduction*, Springer-Verlag Berlin Heidelberg (1996).
[12] C. M. Bishop, *Neural Networks for Pattern Recognition*, Oxford University Press (1995).
[13] L. Lønnblad, C. Peterson, H.Pi and T. Røgnvaldsson, JETNET *3.1 - A Neural Network program for jet discrimination and other High Energy Physics triggering situations*, Department of Theoretical Physics, University of Lund, Sweden (1994).
[14] P. Abreu et al, Nucl. Instr. & Meth. **A427** (1999) 487.
[15] T. Sjöstrand, *PYTHIA 5.7 / JETSET 7.4*, CERN-TH.7112/93 (1993).
[16] K.-H. Becks, J. Drees, U. Flagmeyer and U. Müller, Nucl. Instr. & Meth. **A426** (1999) 599.
[17] S. Catani, G. Turnock and B. R. Webber, Phys. Lett. **B295** (1992) 269.
[18] G. C. Fox and S. Wolfram, Nucl. Phys. **B149** (1979) 413.
[19] L. Lönnblad, Comp. Phys. Comm. **71** (1992) 15.
[20] Particle Data Group, E. Phys. J. **C3** (1998) 1.
[21] DELPHI Collaboration, P. Abreu et al., Phys. Lett. **B439** (1998) 209.
[22] D. Bardin et al., Comp. Phys. Comm. **104** (1997) 161.
[23] ALEPH Collaboration, R. Barate et al., Phys. Lett. **B453** (1999) 107.
[24] L3 Collaboration, M. Acciarri et al., Phys. Lett. **B436** (1998) 437.
[25] OPAL Collaboration, G. Abbiendi et al., Eur. Phys. J. **C8** (1999) 191.